ELSEVIER

Removal of acid blue 062 on aqueous solution using calcinated colemanite ore waste

Necip Atar, Asim Olgun *

Department of Chemistry, Faculty of Arts and Science, University of Dumlupinar, Kütahya, Turkey

Abstract

Colemanite ore waste (CW) has been employed as adsorbent for the removal of acid blue 062 anionic dye (AB 062) from aqueous solution. The adsorption of AB 062 onto CW was examined with respect to contact time, calcination temperature, particle size, pH, adsorbent dosage and temperature. The physical and chemical properties of the CW, such as particle sizes and calcinations temperature, play important roles in dye adsorption. The dye adsorption largely depends on the initial pH of the solution with maximum uptake occurring at pH 1. Three simplified kinetics models, namely, pseudo-first order, pseudo-second order, and intraparticle diffusion models were tested to investigate the adsorption mechanisms. The kinetic adsorption of AB 062 on CW follows a pseudo-second order equation. The adsorption data have been analyzed using Langmuir and Freundlich isotherms. The results indicate that the Langmuir model provides the best correlation of the experimental data. Isotherms have also been used to obtain the thermodynamic parameters such as free energy, enthalpy and entropy of the adsorption of dye onto CW.
© 2006 Elsevier B.V. All rights reserved.

Keywords: Colemanite ore waste; Adsorption; Acidic dye; Isotherms; Langmuir

1. Introduction

In our century, environmental compliance requirements have become increasingly difficult to attain in both wastewater discharge and chemical handling. The main pollution sources of water are dyes and pigments, which are emitted into wastewater from various industrial branches such as dyestuff, textile, leather, paper, etc. Many physical and chemical treatment methods namely adsorption [1], coagulation [2], precipitation, membrane filtration, solvent extraction and chemical oxidation [3] have been used for the treatment of textile effluent. Among these methods, adsorption has been shown to be an effective technique with its efficiency, simplicity of design, and applicability on large scale to treat dyes in more concentrated form [4,5].

The adsorption of dyes on various types of materials has been studied in detail. Activated carbon has been shown as an effective adsorbent with its high surface area and high adsorption capacity [6–8]. However, it has relatively high operation costs and problems with regeneration of the spent carbon hamper its

large-scale application. Therefore, a number of low-cost adsorbents have been examined for the treatment of wastewaters, such as zeolite [9], sepiolite [10,11,5], kaolinite [12], montmorillonite [13], smectite [14], bentonite [15,16], alunite [17,18]. In recent years, considerable experimental progress has been done on the adsorption of dyes on various types of waste materials. These include: coal fly ash [19–21], coal bottom ash [22,23], bagasse fly ash [24], fertilizer waste [25], blast furnace slag [26,27], agricultural waste residues [28,29] and red mud [30].

The present paper is an attempt to explore a possibility to utilize a waste material, colemanite ore waste (CW) to remove a well-known dye, the acid blue 062 anionic dye (AB 062). CW is a waste materials originated in great amounts in enrichment process in boron plant. It is primarily composed of fine particles of silica, calcium, boron, magnesium, iron and potassium oxides. Colemanite ($2CaO2B_2O_3 \cdot 5H_2O$), like other borates, is a complex mineral that is mostly found in Turkey. The basic structure of colemanite contains endless chains of interlocking $BO_2(OH)$ triangles and $BO_3(OH)$ tetrahedrons with the calcium, water molecules and extra hydroxides interspersed between the chains. Although, CW utilization in construction and other engineering materials seems promising, it is unlikely that this will ever use all the CW generated [31–33]. Research is therefore

* Corresponding author. Tel.: +90 274 2652051; fax: +90 274 2652056.
E-mail address: aolgun@dumlupinar.edu.tr (A. Olgun).

needed to develop new alternative applications that can further exploit CW.

The objective of this work is to study the adsorption of AB 062 from aqueous solutions onto CW. The effects of calcinations temperature, contact time, pH, particle size, and concentration on the adsorption of AB 062 onto CW were investigated. Furthermore, the kinetics and thermodynamics data were evaluated.

2. Materials and methods

2.1. Materials

A commercial textile dye AB 062 (purity: 98%) was obtained from Setaş Textile (Istanbul, Turkey) and used without further purification. The chemical structure of AB 062 is given in Fig. 1. The adsorbent used in this work was obtained from Etibor (Kütahya, Turkey). It was ground in a laboratory type ball-mill and sieved to give 30–90, 90–150, 150–315 and 315–500 μm size fractions using ASTM standard sieves. Then the sample was calcined in a Thermolyn 4800 furnace in the temperature range of 473–1073 K.

2.2. Characterization

X-ray diffraction patterns of calcined CW were obtained with a Rikagu Miniflex X-ray diffractometer using monochromatic Cu Kα radiation operating at 30 kV and 15 mA over the range (2θ) of scanning 5–75°. Chemical compositions of raw CW and Calcined CW samples were determined by using XRF spectrometer (Spectro X-Lab). DTA and thermo gravimetric analysis (TG/DTA) of the raw CW sample was obtained using a Perkin Elmer Diamond Simultaneous DTA-TGA apparatus. The samples were heated from 35 to 1100 °C at a constant rate of 10 °C/min in nitrogen gas dynamic atmosphere (100 cm^3/min). The specific surface area of calcined CW samples at different temperatures was determined using a Quantachrome BET apparatus. Scanning electron microscopy (SEM) of selected CW samples and dye adsorbed CW was performed using a ZIS SUPA 50 VP scanning electron microscope.

2.3. Adsorption procedure

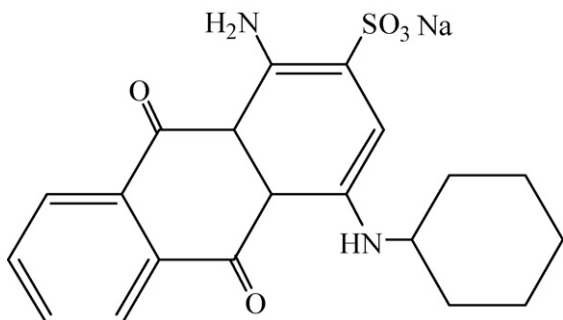A stock solution of AB 062 at a concentration of 100 mg/L was prepared with distilled water. For the particles sizes effect on dye removal, the dye solution (50 ml) was taken in Erlenmeyer flasks and agitated with 0.1 g calcinated CW (30–90 μm size fractions) at room temperature in an IKA magnetic stirrer at 400 rpm for 90 min. The solution pH was adjusted to 1 by adding a small amount of HCl or NaOH (1 M). Calcinated CW samples were analyzed for maximum adsorption capacity. The sample calcinated at 773 K resulted in maximum adsorption. The effects of CW doses on the amount of dye adsorbed were investigated by agitating different amounts of CW (0.5–10 g) with AB 062 solution (100 mg/L). The change of the adsorbance of AB 062 was determined at a certain time intervals (10, 20, 30, 45, 60, 90, 120, 150, and 180 min) during the adsorption process. The equilibrium was established after 90 min. After equilibrium or defined time intervals, the samples were taken from the magnetic stirrer, filtered through a 0.11 μm membrane filter and the filtrate was analyzed for residual dye concentration at the wavelength corresponding to maximum absorbance, λ_{max}, using a spectrophotometer (Shimadzu UV-1700 Double Beam). The influence of pH on dye removal was studied by adjusting dye solutions (100 mg/L) to different pH values (1, 2, 3, 4, 5, 6, 7, 8, 9, and 10) and agitated with 2 g/L of CW for 90 min. The final pH value in each case was measured, followed by analyzing the dye remaining in solution. In order to study the adsorption kinetics 0.1 g of CW were kept in contact with 50 ml of dye solution for 90 min to allow attainment of equilibrium at constant temperatures of 25, 35, 45, and 55 °C.

3. Results and discussion

3.1. Characteristics of adsorbents

Chemical composition of the CW is listed in Table 1. Chemical content of CW mainly are silicon dioxide, calcium oxide, boron oxide, and magnesium oxide. Based on the thermal behavior of the CW with the DTA-TG analysis, it is found that CW loses its crystal water in endothermic reactions between temperatures of 320 and 410 °C (Fig. 2). It is clear from XRD (Fig. 3) and DTA-TG analysis that the decomposition of CW take place at around 600 °C. At this stage, colemanite in the waste is decomposed to B_2O_3 and CaO in their amorphous forms upon calcinations. It should be noted that CW contains some of the other major phases, namely, illit/mica, calcite, feldspar

Fig. 1. Molecular structure of AB 062.

Table 1
Chemical composition of original and calcined CW

Component	Chemical analysis (wt%)	
	Original colemanite waste	Calcined colemanite waste
SiO$_2$	26.45	27.52
Al$_2$O$_3$	3.66	3.82
Fe$_2$O$_3$	1.87	2.15
CaO	18.53	23.17
MgO	8.94	9.76
SO$_3$	0.92	0.694
K$_2$O	1.71	1.89
B$_2$O$_3$	17.25	18.10

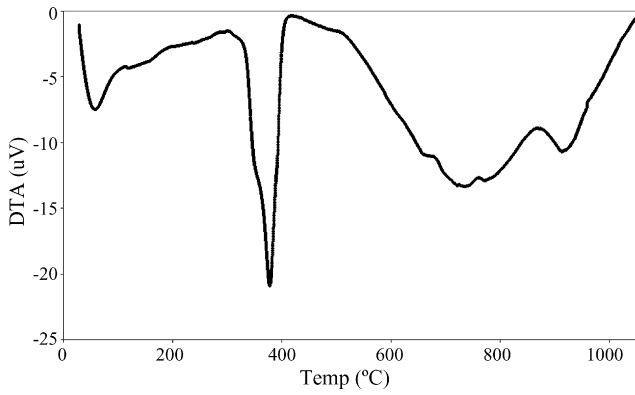Fig. 2. DTA thermograms of CW.

Fig. 4. Effect of pH on the removal of AB 062 by calcined CW.

and smectite. After heating the peak intensity of the illit/mica and feldspar are significantly reduced and the smectite peak disappears.

3.2. Effect of pH

The pH of the solutions plays an important role in the whole adsorption process and particularly on the adsorption capacity. The variation of AB 062 adsorption on the over broad range of pH is shown in Fig. 4. As shown, the adsorption is lower at pH higher than 7 and then is increased to higher values at pH lower than 7. More significant enhancement in the adsorption of dye is reached at pH 1. It is well known that ionic dyes upon dissolutions release coloured dye anions/cations into solutions. The adsorption of these charged dye groups onto an adsorbed surface is influenced by the surface charge on the adsorbent. At lower pH value more protons will be available to protonate the adsorbent surface, thereby increa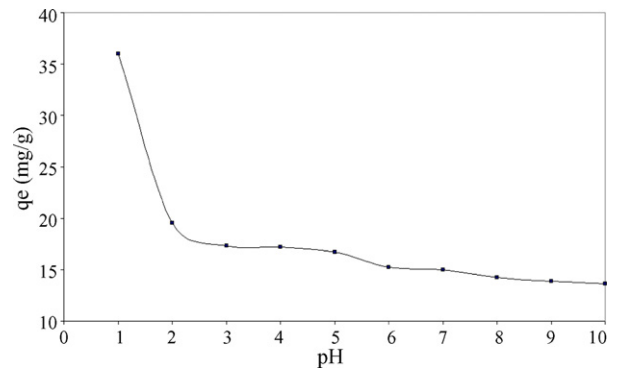sing the electrostatic attractions between negatively charged dye anions and positively charged adsorption sites and causing an increase in the dye adsorption [1]. As the pH of the system increases, the number of positively charged sites at the oxide/solution interface decreases, and the number of the negatively charged sites increases. A negative charged surface site on the CW does not favour the adsorption of anionic dye due to electrostatic repulsion. This result is consistent with the earlier findings [34]. It is worth mentioning that the concentration of acid solution must be kept at a certain level due to solubility of colemanite. Earlier studies shown that the dissolution of the colemanite in HCl solution increases with the increasing solution concentration and temperature, and that solubility of colemanite is maximum in 5% HCl solution [35]. In the present study, we did not detect any boron impurity present in the solution over a wide pH range of 1–10. The further decrease in the pH of the solutions slightly affected the dissolution of colemanite. Hence, the values obtained from the adsorption of dye at pH 1 were not given in the present study.
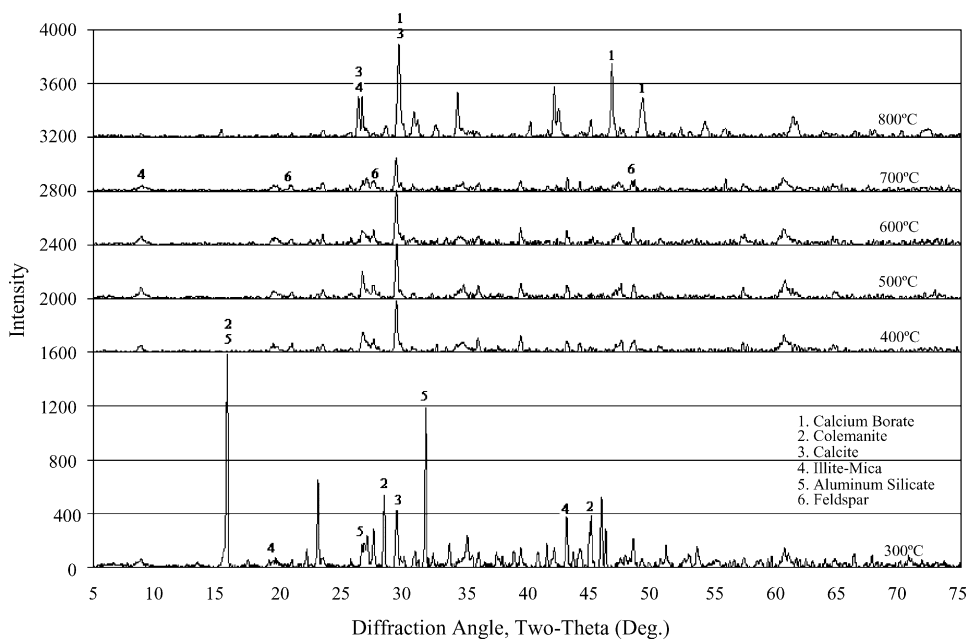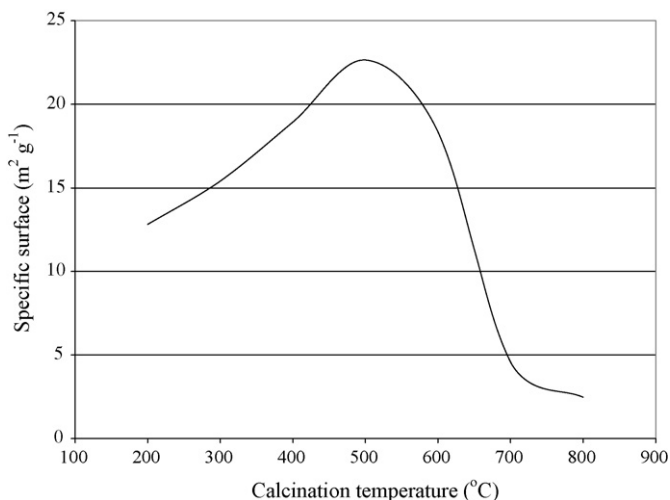

Fig. 3. XRD patterns of CW at various temperatures.

Fig. 5. The specific surface area of the CW heated at different temperatures.

3.3. Effect of particle size and adsorbent dosage

The effect of the heat treatment on the specific surface area of CW is given in Fig. 5. As can be observed, the specific surface area of CW increases up to a temperature of 500 °C, and then it starts to decrease with increasing temperature. The change in the surface are of the CW may be attributed to the dehydration process of colemanite. Water molecules formed by broken-away OH groups and those separated from the borate changes fills the free spaces between the borate chains. With increasing temperature the pressure of the enclosed water molecules increases so much that it disrupts the framework. Thus, the enclosed water molecules are released increasing the number of the pores in the sample. Accordingly, specific surface of the sample increases. Upon heating beyond 500 °C, the specific surface area of CW decreases probably due to decomposition of colemanite [36]. The effect of particle size of on the removal of AB 062 by CW calcinated at 500 °C is given in Fig. 6. As seen, the adsorption capacity for AB 062 increases with the decreasing particles sizes. The relative increases in adsorption with particles of smaller sizes may be attributed to the fact that they have a larger surface area. Small particles will have a shorter diffusion path, thereby
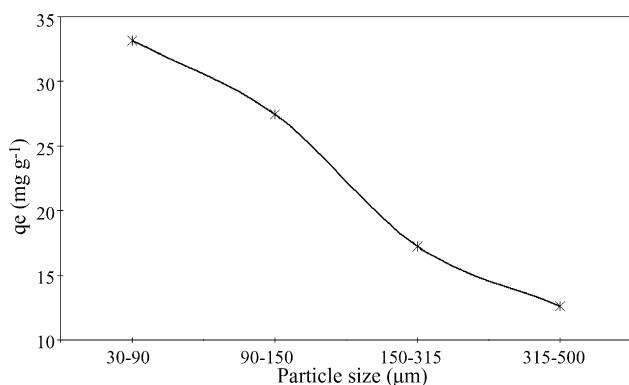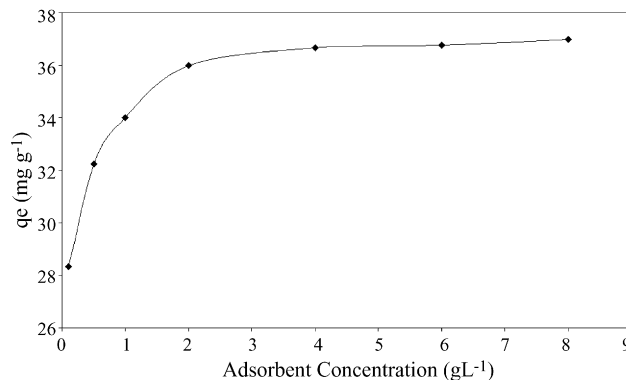

Fig. 7. Effect of adsorbent dosage on the removal of AB 062 by calcined CW.

allowing dye molecules to penetrate all the initial pore structure of the calcinated CW.

The effect of CW doses on the amount of dye adsorbed is given in Fig. 7. The results indicate that the uptake of the dye by CW significantly increases with the increasing adsorbent content up to a dosage of 2 g/L and then it slow down. The dye removal of CW was found to be negligible after dosage of 2 g/L. then used for all further studies.

3.4. Effect of calcination temperature

The effect of calcination temperature on the adsorption of AB 062 by CW is shown in Fig. 8. The adsorption of dye on CW gradually increases with increasing calcinations temperature and reaches a maximum at 500 °C and then it starts to decrease. This result may be attributed to presence of the colemanite impurity in CW. It has been stated that colemanite contains chains of interlocking $BO_2(OH)$ triangles and $BO_3(OH)$. Tetrahedrons with the calciums, water molecules and extra hydroxides interspersed between the chains [37]. The loss of the water molecules and decomposition of the hydroxyl groups, which are mainly effective sites for adsorption, with increasing temperature will affect the specific surface area and adsorption capacity of CW. As AB 062 is an anionic dye, a decrease in the number of the hydroxyl groups leads to high adsorption capacity of CW.

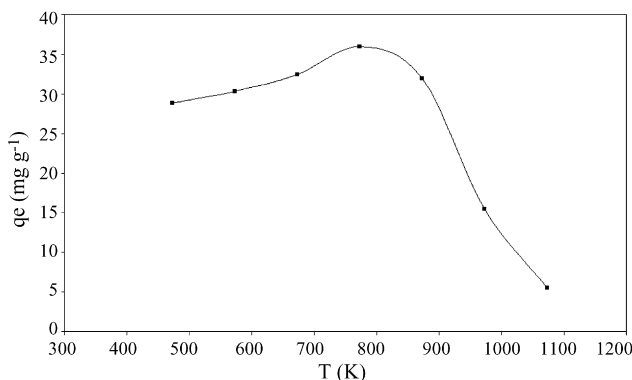Fig. 6. Effect of particle size on the removal of AB 062 by calcined CW.

Fig. 8. Effect of calcination temperature on the removal of AB 062 by calcined CW.
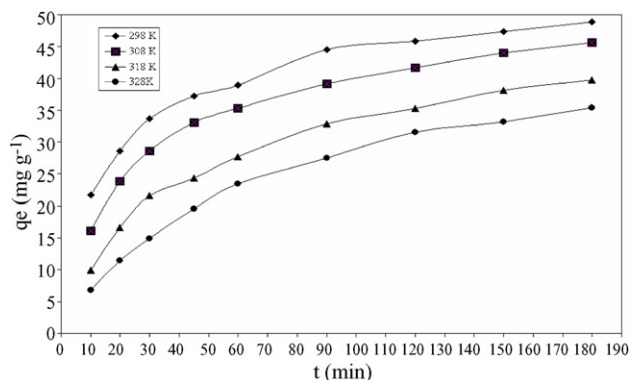
Fig. 9. Effect of contact time on the removal of AB 062 by calcined CW at various temperatures.

3.5. Effect of contact time

The effect of contact time on the amount of dye adsorbed onto CW at various temperatures is presented in Fig. 9. The dye concentrations in solution were determined at different times. All the experiments were conducted at pH 1. The plots representing adsorption of dye on the CW, visualize two distinct phases: the first phase indicates the instantaneous adsorption of the dye within 90 min of contact time, the second one shows a gradual equilibrium. Maximum adsorption of AB 062 was observed at 120 min. After this time, adsorption rate was slow leading to a single, smooth, and continuous saturation curve.

3.6. Effect of temperature

The effect of temperature on adsorption was studied by carrying out a series of isotherms at 25, 35, 45, and 55 °C for CW as shown in Fig. 9. The uptake of the AB 062 by CW decreases with increasing temperature, which indicates the exothermic nature of the adsorption process. This result may be attributed to the enhanced mobility of AB 062 ions at high temperature due to greater vibrational energies of the molecules [38]. The Similar temperature effects on the adsorption of acid blue 193 dye onto sepiolite had been observed by Özcan et al. [5].

3.7. SEM analysis

SEM gives a sufficient general overview of the surface morphology and fundamental physical properties of the adsorbent. The CW has a variable surface intersected by pores, the surface being comprised of smooth and angular particles (Fig. 10). From the figure, it is clear that there is a good possibility for dye to be trapped and adsorbed into these pores and on the rough surface. The SEM pictures of CW samples shows dye staying on the surface with open pores still visible (Fig. 11).

3.8. Adsorption kinetics

In order to study the rate determining step for the adsorption of AB 062 on CW, three kinetics models were tested to fit the experimental data obtained from dye removal study. The kinetic
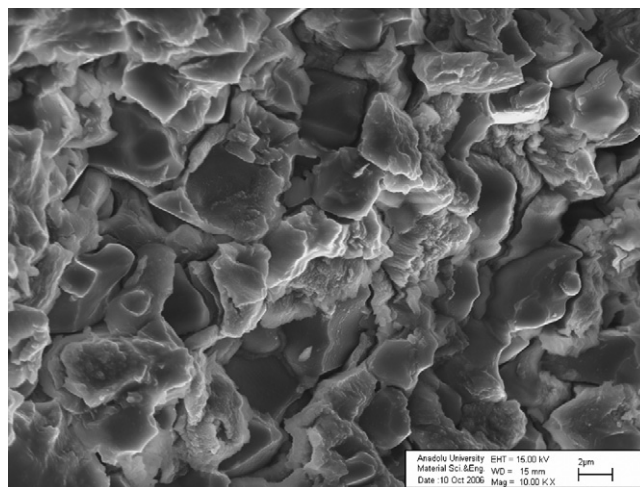

Fig. 10. SEM image of CW calcinated at 500 °C.

data were initially fitted with the first-order rate expression [39] given as:

$$\frac{1}{q_t} = \left(\frac{k_1}{q_1}\right)\left(\frac{1}{t}\right) + \frac{1}{q_1} \tag{1}$$

where q_1 and q_t are the amount of dye adsorbed on adsorbed per unit mass of the adsorbent (mg/g) at equilibrium and time t, respectively, and k is the rate constant of adsorption (min^{-1}).

The pseudo-second order model [40] can be expressed as:

$$\frac{t}{q_t} = \frac{1}{k_2 q_2^2} + \frac{1}{q_2}t \tag{2}$$

where q_2 is the maximum adsorption capacity (mg g^{-1}); k_2 the rate constant of the pseudo-second order equation (g mg^{-1} min^{-1}); q_t is the amount of dye adsorbed on adsorbed per unit mass of the adsorbent (mg/g).

The interparticle diffusion equation [41] is

$$q_t = k_p t^{1/2} + C \tag{3}$$

where C is the intercept, k_p the intraparticle diffusion rate constant.
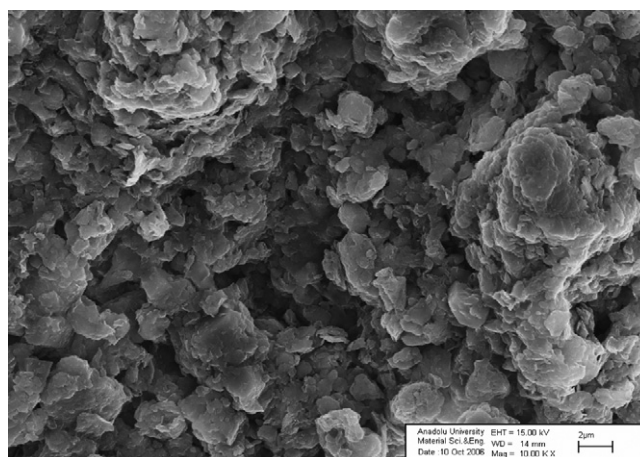

Fig. 11. SEM image of dye adsorbed CW calcinated at 500 °C.

Table 2
Kinetic parameters for the adsorption of AB 062 onto calcined CW at various temperatures

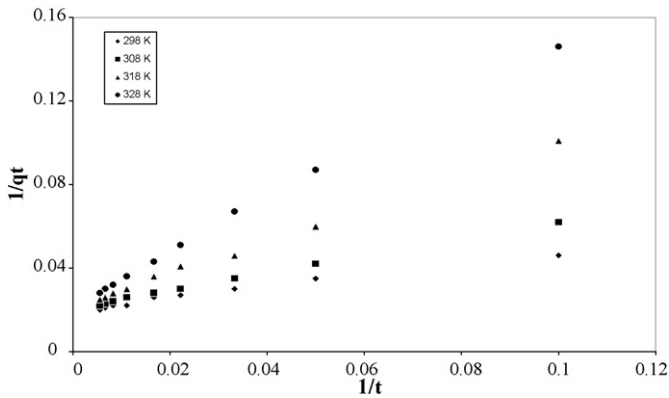| T (K)	q_{exp} (mg g^{-1})	k_1 (min^{-1})	q_1 (mg g^{-1})	r_1^2	k_2 (g mg^{-1} min^{-1})	q_2 (mg g^{-1})	r_2^2	k_p (mg g^{-1} min$^{-1/2}$)	C (mg g^{-1})	r_p^2
298	48.89	13.61	50.00	0.979	1.06×10^{-3}	53.19	0.999	2.49	18.13	0.930
308	45.60	20.28	48.54	0.998	8.22×10^{-4}	50.76	0.998	2.67	12.28	0.940
318	39.74	37.23	46.94	0.998	5.16×10^{-4}	48.08	0.998	2.80	4.46	0.967
328	35.41	55.96	44.64	0.998	3.37×10^{-4}	47.39	0.999	2.81	0.34	0.980

Fig. 12. First-order kinetic plots for the adsorption of AB 062 onto calcined CW at various temperatures.

Figs. 12 and 13 show the curve-fittings plots of the first-order rate and the pseudo-second order reactions, respectively, and the parameters obtained for the three models are presented in Table 2. As shown, the kinetics data do not fit the first order equation. Good correlation coefficients were obtained by fitting the experimental data to Eq. (2), indicating that the adsorption process on AB 062 is pseudo-second order as shown in
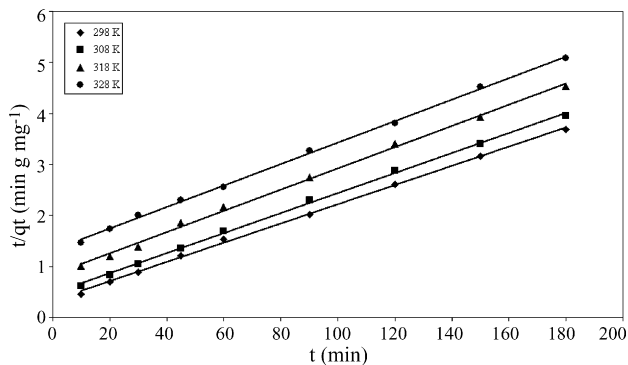

Fig. 13. Pseudo-second order kinetic plots for the adsorption of AB 062 onto calcined CW at various temperatures.
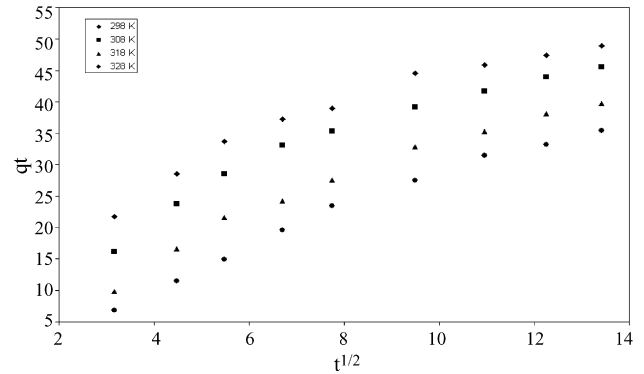

Fig. 14. Interparticle diffusion model plots for the adsorption of AB 062 onto calcined CW at various temperatures.

Fig. 13. The pseudo-second order rate constants indicate a steady decease from 1.06×10^{-3} to 3.37×10^{-4} g mg^{-1} min^{-1} with an increase in the solution temperatures from 25 to 55 °C (Table 2). The values of rate constant demonstrate that adsorption of AB 062 depends on the temperature of the solution. Increasing the temperature of the solution increases the rate of the approach to the equilibrium but decreases equilibrium adsorption capacity. This result may be attributed to the molecular motion of the adsorbed molecules on the adsorbent surface. At high temperature, adsorbed molecules have greater vibrational energies that may results in a breaking of Van der Waals or hydrogen bonds [42].

In a liquid–solid system, the fractional uptake of the solute on particles varies according to a function of $[(D_t)^{0.5}/r]$, where D is the diffusivity within the particle and r is the particle radius. The initial rates of intraparticle diffusion are obtained by linearization of the curve $q_t = f(t^{1/2})$. In the present study, the plot of q_t versus $t^{1/2}$ presents a multi-linearity, which indicates that two or more steps occur in the adsorption process (Fig. 14). The slope of the line in each stage is written as the rate parameter. The initial linear portion of the plots is the gradual adsorption stage, where the intraparticle diffusion is rate-controlled. The second portion is the final equilibrium stage, where the intraparticle

Table 3
Adsorption isotherm constants for the adsorption of AB 062 onto calcined-colemanite waste at various temperatures

T (K)	Langmuir				Freundlich		
	q_{max} (mol g^{-1})	K_L (L mol^{-1})	r_L^2	R_L	$1/n$	K_F (L g^{-1})	r_F^2
298	3.80×10^{-4}	2.84×10^3	0.999	0.332	0.649	3.25×10^{-2}	0.984
308	5.43×10^{-4}	1.46×10^3	0.998	0.330	0.763	7.69×10^{-2}	0.986
318	5.34×10^{-4}	1.11×10^3	0.997	0.560	0.787	7.71×10^{-2}	0.979
328	5.77×10^{-4}	0.69×10^3	0.997	0.372	0.840	8.74×10^{-2}	0.994

diffusion starts to slow down due to the extremely low solute concentration in solution. The correlation coefficients calculated for the intraparticle diffusion model (r_p^2) were between 0.930 and 0.980 indicating that the adsorption of AB 062 onto CW may be followed by an intraparticle diffusion up to 90 min.

3.9. Adsorption isotherms

The equilibrium data is very important in optimizing the design parameters for any adsorption system and provide sufficient information on the physicochemical data in evaluating the adsorption process as a unit operation. The distributions of solutes between the liquid phase and solid adsorbent are a measure of the position of equilibrium and can be generally expressed by two equations, namely the Freundlich [43] and the Langmuir [44] isotherm equations which can be expressed in linear forms as

$$\ln q_e = \ln K_F + \frac{1}{n} \ln C_e \tag{4}$$

$$\frac{1}{q_e} = \frac{1}{q_{max}} + \left(\frac{1}{q_{max} K_L} \right) \frac{1}{C_e} \tag{5}$$

where q_e is the equilibrium dye concentration on the adsorbent (mol g^{-1}); C_e, the equilibrium dye concentration in solution (mol L^{-1}); q_{max}, the monolayer capacity of the adsorbent (mol g^{-1}); K_F, the Freundlich constant; K_L, the Langmuir constant; n the heterogeneity factor.

The equilibrium data for adsorption of AB 062 dye onto CW was fitted with Eqs. (4) and (5) and the fitted models along with the experimental data for comparison are shown in Figs. 15 and 16. The fitted adsorption parameters of each isotherm model and their corresponding error function are reported in Table 3. It is evident from r^2 values that the equilibrium data of the system was well explained by the Langmuir model when compared to the Freundlich model. The slope $1/n$ ranging 0–1, is a measure of adsorption intensity or surface heterogeneity, becoming more heterogeneous as its value gets closer to zero. In the present study the $1/n$ values obtained indicates a normal Langmuir isotherm. The equilibrium parameter (R_L) obtained vary between 0.330 and 0.560 and also indicate the favorable uptake of AB 062 by CW [16].
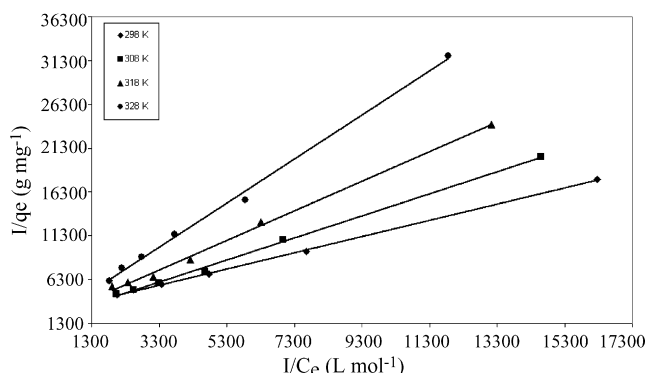

Fig. 15. Langmuir plots for the adsorption of AB 062 onto calcined CW at various temperatures.
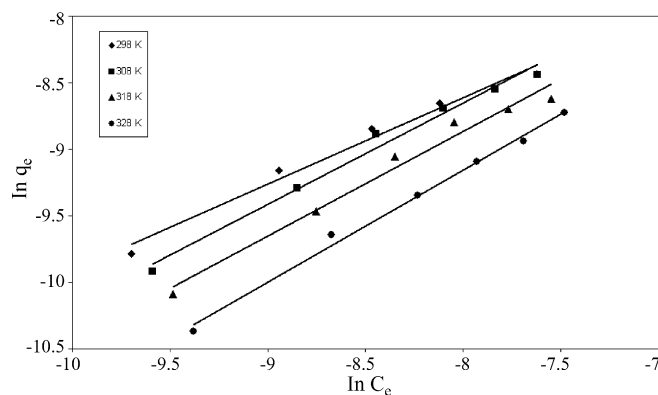

Fig. 16. Freundlich plots for the adsorption of AB 062 onto calcined CW at various temperatures.
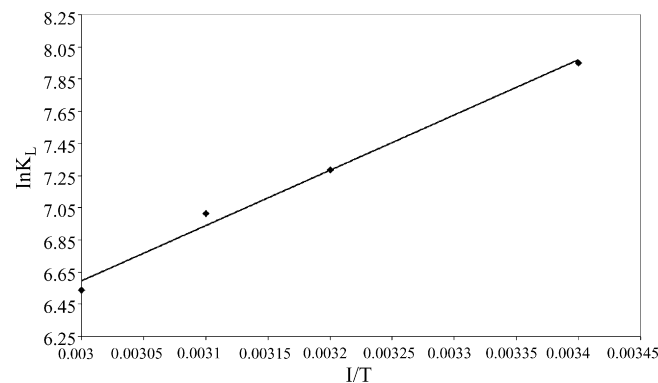

Fig. 17. Plot of ln K_L vs. 1/T for estimation of thermodynamic parameters.

3.10. Thermodynamics parameters

The model parameters from the Langmuir isotherm can be used to estimate thermodynamics parameters, that is, standard free energy (ΔG°), standard enthalpy (ΔH°), and standard entropy(ΔS°).

They are expressed as

$$\Delta G^\circ = -RT \ln K_L \tag{5}$$

$$\ln K_L = -\frac{\Delta H^\circ}{RT} + \frac{\Delta S^\circ}{R} \tag{6}$$

where K_L is the Langmuir constant. The plot of the K_L as a function of 1/T a straight line from which ΔH° and ΔS° were calculated from the slope and intercept, respectively. The result presented in Fig. 17 and Table 4 show that the standard free energy change during adsorption process is between −2.587 and 1.012 kJ mol^{-1}, indicating that the adsorption process is spontaneous AB 062 with a high affinity on CW and that the system does gain energy from an external source at high temperatures.

Table 4
Thermodynamic parameters

T (K)	ΔG° (kJ mol^{-1})	ΔH° (kJ mol^{-1})	ΔS° (J mol^{-1} K^{-1})	r^2
298	−2.587	−28.64	−31.10	0.991
308	−0.970			
318	−0.276			
328	1.012			

The change in enthalpy was found to be negative (Table 4). The negative values confirm the exothermic nature of the adsorption. The negative values of the entropy change show decreased randomness at the solid-solution interface with some structural changes in the adsorbate and adsorbent. The decrease in the dye adsorption with increasing temperature might also be due to the reduced rate of intraparticle diffusion of the adsorbate, as diffusion is an exothermic process.

4. Conclusions

CW has been investigated for removal of AB 062 from aqueous solution. The CW had high adsorption capacities to remove the anionic dye, whose maximum monolayer adsorption capacity is 48.885 mg g^{-1} at pH 1, 25 °C. The adsorption capacities were significantly affected by the initial dye concentration, pH, and calcinations temperature. The adsorption capacity of CW decreased with the increasing solutions pH. The uptake of the dye also increases with the increasing calcination temperatures up to 500 °C, and then it started to decrease due to sintering effect.

The adsorption isotherm data were well fitted by the Langmuir model while the pseudo-second order kinetic model represented the kinetic data.

The higher adsorption capacity of 48.885 mg g^{-1} for CW shows that the calcinated CW could be used as an adsorbent for the removal of acid dyes. Further study is under investigation to develop a suitable regeneration method to reuse CW for multi-operational cycles.

References

[1] M.S. Chiou, G.S. Chuang, Competitive adsorption of dye metanil yellow and RB15 in acidic solutions on chemically cross-linked chitosan beads, Chemosphere 62 (2006) 731–740.

[2] R.J. Stephenson, J.B. Sheldon, Coagulation and precipitation of mechanical pulping effluent. 1. Removal of carbon and turbidity, Water Res. 30 (1996) 781–792.

[3] I.A. Salem, M. El-maazawi, Kinetics and mechanism of color removal of methylene blue with hydrogen peroxide catalysed by some supported alumina surfaces, Chemosphere 41 (2000) 1173–1180.

[4] S. Wang, Y. Boyjoo, A. Choueib, Z.H. Zhu, Removal of dyes from aqueous solution using fly ash and red mud, Water Res. 39 (2005) 129–138.

[5] A. Özcan, E.M. Öncü, A.S. Özcan, Kinetics, isotherm and thermodynamic studies of adsorption of Acid Blue 193 from aqueous solutions onto natural sepiolite, Colloid Surf. A: Physicochem. Eng. Aspects 277 (2006) 90–97.

[6] N. Kanan, M.M. Sundaram, Kinetics and mechanism of removal of methylene blue by adsorption on various carbon—a comparative study, Dyes Pigments 51 (2001) 25–40.

[7] P.K. Malik, Use of activated carbons prepared from sawdust and rice-husk for adsorption of acid dyes: a case study of acid yellow 36, Dyes Pigments 56 (2003) 239–249.

[8] V.K. Gupta, K. Suresh, D. Mohan, S. Mohan, Equilibrium uptake, sorption dynamics optimization, and column operations for the removal and recovery of malachite green from waste water using activated carbon and activated slag, Ind. Eng. Chem. Res. 36 (1997) 2207–2218.

[9] B. Armağan, M. Turan, M.S. Çelik, Equilibrium studies on the adsorption of reactive azodyes into zeolite, Desalination 170 (2004) 33–39.

[10] M. Alkan, S. Çelikçapa, Ö. Demirbaş, M. Doğan, Removal of reactive blue 221 and acid blue 62 anionic dyes from aqueous solutions by sepiolite, Dyes Pigments 65 (2005) 251–259.

[11] A. Özcan, E.M. Öncü, A.S. Özcan, Adsorption of acid blue 193 from aqueous solutions onto DEDMA, sepiolite, J. Hazard. Mater. B129 (2006) 244–252.

[12] R.G. Haris, J.D. Wells, B.B. Jhonson, Selective adsorption of dyes and other organic molecules to kaolinite and oxide surfaces, Colloid Surf. A: Physicochem. Eng. Aspects 180 (1–2) (2001) 131–140.

[13] C.C. Wang, L.C. Juang, T.C. Hsu, C.K. Lee, F.C. Huang, Adsorption of basic dyes onto montmorillonite, J Colloid Interface Sci. 273 (1) (2004) 80–86.

[14] M. Ogawa, R. Kawai, K. Kuroda, Adsorption and aggregation of cationic cyanine dye on smectites, J. Phys. Chem. US 100 (40) (1996) 16218–16221.

[15] A.S. Özcan, A. Özcan, Adsorption of acid dyes from aqueous solutions onto acid activated bentonite, J Colloid Interface Sci. 276 (1) (2004) 39–46.

[16] P. Baskaralingam, M. Pulikesi, D. Elango, D. Elango, V. Ramamurthi, S. Sivanesan, Adsorption of acid dye onto organobentonite, J. Hazard. Mater. B128 (2006) 138–144.

[17] S. Tunalı, A.S. Özcan, A. Özcan, T. Gedikbey, Kinetics and equilibrium studies for the adsorption of Acid Red 57 from aqueous solutions onto calcinated-alunite, J. Hazard. Mater., 2006, in press.

[18] M. Özacar, İ.A. Şengil, Adsorption of reactive dyes on calcined alunite from aqueous solutions, J. Hazard. Mater. B98 (2003) 211–224.

[19] P. Janos, H. Buchtova, M. Ryznarova, Sorption of dyes from aqueous solutions onto fly ash, Water Res. 37 (2003) 4938–4944.

[20] K.R. Ramakrihna, T. Viraraghavan, Dye removal using low cost adsorbent, Water Sci. Technol. 36 (1997) 189–196.

[21] K. Ravikumar, S. Ramalingam, S. Krishnan, K. Balu, Application of response surface methodology to optimize the process variables for reactive red and acid brown dye removal using a novel adsorbent, Dyes Pigments 70 (2006) 18–26.

[22] V.K. Gupta, A. Mittal, L. Krishnan, V. Gajbe, Adsorption kinetics and column operations for the removal and recovery of malacjite green from waste water using bottom ash, Sep. Purif. Technol. 40 (2004) 87–96.

[23] V.K. Gupta, A. Mittal, V. Gajbe, Adsorption and desorption studies of a water soluble dye, Quinoline Yellow, using waste materials, J Colloid Interface Sci. 284 (2005) 89–98.

[24] V.K. Gupta, D. Mohan, S. Sharma, M. Sharma, Removal of basic dyes (Rhodamine B and Methylene blue) from aqueous solutions using bagasse fly ash, Sep. Sci. Technol. 35 (2000) 2097–2113.

[25] A.K. Jain, V.K. Gupta, A. Bhatnagar, Suhas, Utilization of industrial waste products as adsorbents for the removal of dyes, J. Hazard. Mater. B101 (2003) 31–42.

[26] V.K. Gupta, I. Ali, Suhas, D. Mohan, Equilibrium uptake and sorption dynamics for the removal of basic dye (basic red) using low-cost adsorbents, J. Colloid Interface Sci. 265 (2003) 257–264.

[27] K.R. Ramakrishna, T. Viraraghavan, Use of slag for dye removal, Waste Manage. 17 (1998) 483–488.

[28] A. Mittal, L. Krishnan, V.K. Gupta, Removal and recovery of malachite green from wastewater using and agricultural waste material, de-oiled soya, Sep. Purif. Technol. 43 (2005) 125–133.

[29] A. Mittal, L. Kurup (Krishnan), V.K. Gupta, Use of waste materials-bottom ash and de-oiled soya, as potential adsorbents for the removal of Amaranth from aqueous solutions, J. Hazard. Mater. B117 (2005) 171–178.

[30] V.K. Gupta, S. Suhas, I. Ali, V.K. Saini, Removal of Rhodamine B, Fast green, and methylene blue from wastewater using red mud an aluminum industry waste, Ind. Eng. Chem. Res. 43 (2004) 1740–1747.

[31] I. Kula, A. Olgun, Y. Erdogan, V. Sevinc, Effects of colemanite waste, coal bottom ash and fly ash on the properties of cement, Cem. Concr. Res. 31 (2001) 491–494.

[32] Ş. Targan, A. Olgun, Y. Erdoğan, V. Sevinç, Influence of natural pozzolan, colemanite ore waste, bottom ash, and fly ash on the properties of portland cement, Cem. Concr. Res. 33 (2003) 1175–1182.

[33] A. Olgun, Y. Erdogan, Y. Ayhan, B. Zeybek, Development of ceramic tiles from coal fly ash and tincal ore waste, Ceram. Int. 31 (2005) 153–158.

[34] M.S. Celik, M. Hancer, J.D. Miller, Flotation chemistry of boron minerals, J. Colloid Interface Sci. 256 (2002) 121–131.

[35] V.M. Imamutdinova, Mechanism of solution of native borates in HCl solution, Zh. Prikl. Khim 37 (1963) 1095–1099.

[36] Ö Yildiz, The effect of heat treatment on colemanite processing: a ceramic application, Powder Technol. 142 (2004) 7–12.

[37] I. Waclawska, L. Stoch, J. Paulık, F. Paulık, Thermal decomposition of colemanite, Thermochim. Acta 126 (1988) 307–318.

[38] K. Ravikumar, B. Deebika, K. Balu, Decolourization of aqueous dye solutions by a novel adsorbent: Application of statistical designs and surface plots for the optimization and regression analysis, J. Hazard. Mater. B1222 (2005) 75–83.

[39] N. Kannan, M.M. Susndaram, Kinetics and mechanism of removal of methylene blue by adsorption on various carbons—a comparative study, Dyes Pigments 51 (2001) 25–40.

[40] Y.S. Ho, G. McKay, Kinetic models for the sorption of dye from aqueous solution by wood, Process. Saf. Environ. Protect. 76 (1998) 183–191.

[41] W.J. Weber Jr., J.C. Morriss, Kinetics of adsorption on carbon from solution, J. Sanitary Eng. Div. Am. Soc. Civil Eng. 89 (1963) 31–60.

[42] M. Khalfaoui, M.H.V. Baouab, R. Gauthier, A. Ben Lamine, Acid dye adsorption onto cationized polyamide fibers. Modeling and consequent interpretations of model parameter behaviors, J. Colloid Interface Sci. 296 (2006) 419–427.

[43] H.M.F. Freundlich, Über die adsorption in LÖsungen, C. Phys. Chem. 57 (1906) 385–470.

[44] I. Langmuir, The adsorption of gases on plane surfaces of glass, mica and platinum, J. Am. Chem. Soc. 40 (1918) 1361–1403.